Construction of Metal Butterflies on a Metallacarborane Scaffold. 2. Synthesis and Structures of Hetero-tri- and -tetrametallic Clusters

Thomas D. McGrath,* Shaowu Du, Bruce E. Hodson, and F. Gordon A. Stone*

Department of Chemistry & Biochemistry, Baylor University, Waco, Texas 76798-7348

Received May 15, 2006

Treatment of $[N(PPh_3)_2][1,3,6\text{-}\{Re(CO)_3\}\text{-}3,6\text{-}(\mu\text{-}H)_2\text{-}1,1\text{-}(CO)_2\text{-}2\text{-}Ph\text{-}closo\text{-}1,2\text{-}IrCB_9H_7]$ (**2a**) with $\{Cu(PPh_3)\}^+$ gives two types of polymetallic species: $[1,4,7\text{-}\{Cu(PPh_3)\}\text{-}1,5,6\text{-}\{Re(CO)_3\}\text{-}4,5,6,7\text{-}(\mu\text{-}H)_4\text{-}1,1\text{-}(CO)_2\text{-}2\text{-}Ph\text{-}closo\text{-}1,2\text{-}IrCB_9H_5]$ (**4a**), containing a V-shaped Re−Ir−Cu trimetallic unit, and $[1,3,6\text{-}\{Cu_2(PPh_3)_2\}\text{-}3,6\text{-}(\mu\text{-}H)_2\text{-}1,1\text{-}(CO)_2\text{-}2\text{-}Ph\text{-}closo\text{-}1,2\text{-}IrCB_9H_7]$ (**5a**), containing an $IrCu_2$ triangle. In contrast, $[N(PPh_3)_2][1,3,6\text{-}\{Re(CO)_3\}\text{-}3,6\text{-}(\mu\text{-}H)_2\text{-}1,1\text{-}(CO)_2\text{-}2\text{-}Ph\text{-}closo\text{-}1,2\text{-}RhCB_9H_7]$ (**2b**) with the same copper cation essentially affords only the corresponding $RhCu_2$ species **5b**. Reaction of **2a** with $\{Au(PPh_3)\}^+$ yields up to three types of polymetallic species, namely, $[1,6\text{-}\{Au_2(PPh_3)_2\}\text{-}6\text{-}(\mu\text{-}H)\text{-}1,1\text{-}(CO)_2\text{-}2\text{-}Ph\text{-}closo\text{-}1,2\text{-}IrCB_9H_8]$ (**7a**), which contains an $IrAu_2$ triangle and is thus related to compounds **5**, $[1,3,6\text{-}\{Au_2(PPh_3)_2Re(CO)_3\}\text{-}6\text{-}(\mu\text{-}H)\text{-}1,1\text{-}(CO)_2\text{-}2\text{-}Ph\text{-}closo\text{-}1,2\text{-}IrCB_9H_7]$ (**8a**), in which there is an $\{Au_2IrRe\}$ "butterfly" arrangement of metal atoms that is supported by the carborane, and the tetrametallic $[1,3\text{-}\{Au_3(PPh_3)_3\}\text{-}1,1\text{-}(CO)_2\text{-}2\text{-}Ph\text{-}closo\text{-}1,2\text{-}IrCB_9H_8]$ (**9a**), which contains an Au_3 triangle bonded to the iridacarborane. The parallel reaction of **2b** with $\{Au(PPh_3)\}^+$ gives up to four polymetallic products: these are compounds **7b**, **8b**, and **9b**, the rhodium-containing analogues of **7a**, **8a**, and **9a**, respectively, along with the trimetallic $[8,9,10\text{-}endo\text{-}\{Au(PPh_3)\}\text{-}3,4,8\text{-}exo\text{-}\{Re(CO)_3\}\text{-}3,4\text{-}(\mu\text{-}H)_2\text{-}8,8\text{-}(CO)_2\text{-}7\text{-}Ph\text{-}nido\text{-}8,7\text{-}RhCB_9H_7]$ (**6b**), which has a V-shaped Re−Rh−Au unit and a *nido*-structured rhodacarborane core.

Introduction

We have for some time been investigating the chemistry of metal−monocarbollide complexes and, in particular, have taken advantage of the often anionic nature of these species to prepare bi- or polymetallic compounds by reaction with simple cationic transition metal fragments.[1] Although at first such studies were essentially limited to 12-vertex $\{MCB_{10}\}$ species derived from the corresponding long-known[2] $\{CB_{10}\}$ carboranes, recent developments in the synthesis of smaller monocarboranes[3] have allowed access to sub-icosahedral metal−monocarbollide complexes and thence to their polymetallic derivatives. Among the latter class, we have prepared $\{MCB_9\}$ (M = Re,[4] Mn,[5] Mo[6]), $\{Co_2CB_9\}$,[7] $\{MCB_8\}$ (M = Fe,[8] Co[7]), $\{FeCB_7\}$,[9] and $\{M_2CB_7\}$ (M = Fe,[9] Co[7]) species and have demonstrated that many of these clusters add an additional metal center upon treatment with a suitable cationic moiety.

In the preceding paper,[10] we focused on $\{MCB_9\}$ species, specifically $[N(PPh_3)_2][NEt_4][1,1,1\text{-}(CO)_3\text{-}2\text{-}Ph\text{-}closo\text{-}1,2\text{-}MCB_9H_9]$ (M = Mn (**1a**), Re (**1b**); see Chart 1), and described their reactions with sources of the cations $\{M'(CO)_2\}^+$ (M′ = Ir, Rh) to afford the bimetallic species $[N(PPh_3)_2][1,3,6\text{-}\{M(CO)_3\}\text{-}3,6\text{-}(\mu\text{-}H)_2\text{-}1,1\text{-}(CO)_2\text{-}2\text{-}Ph\text{-}closo\text{-}1,2\text{-}M'CB_9H_7]$ (M = Re, M′ = Ir (**2a**), Rh (**2b**); M = Mn, M′ = Ir (**2c**), Rh (**2d**)). In these latter products, the $\{M(CO)_3\}$ fragment, formerly a cluster vertex, has assumed an *exo*-polyhedral role, while the incoming $\{M'(CO)_2\}$ units now occupy a site within the cluster. The metallacarborane anions of compounds **2**, as they retain a negative charge, are attractive substrates for reaction with a further transition metal monocation to obtain heterotrimetallic species. Such reactions, using copper− and gold−phosphine cations, to give tri- and even tetrametallic products, are the subject of this report. A preliminary account has already been made of the reaction of **2a** with sources of $\{Cu(PPh_3)\}^+$ and $\{Au(PPh_3)\}^+$.[11] (In that earlier report, the anion of **2a** was incorrectly formulated as a rhenacarborane bearing an *exo*-polyhedral iridium fragment, and hence its copper and gold derivatives were also erroneously described with rhenacarborane cores. The compounds discussed herein have the correct metal atom assignments.[10])

* To whom correspondence should be addressed. E-mail: tom_mcgrath@baylor.edu; gordon_stone@baylor.edu.

(1) (a) McGrath, T. D.; Stone, F. G. A. *J. Organomet. Chem.* **2004**, *689*, 3891. (b) McGrath, T. D.; Stone, F. G. A. *Adv. Organomet. Chem.* **2005**, *53*, 1.

(2) (a) Hyatt, D. E.; Owen, D. A.; Todd, L. J. *Inorg. Chem.* **1966**, *5*, 1749. (b) Knoth, W. *J. Am. Chem. Soc.* **1967**, *89*, 1274.

(3) (a) Brellochs, B. In *Contemporary Boron Chemistry*; Davidson, M. G., Hughes, A. K., Marder, T. B., Wade, K., Eds.; Royal Society of Chemistry: Cambridge, U.K., 2000; p 212. (b) Stíbr, B.; Tok, O. L.; Milius, W.; Bakardjiev, M.; Holub, J.; Hnyk, D.; Wrackmeyer, B. *Angew. Chem., Int. Ed.* **2002**, *41*, 2126. (c) Franken, A.; Kilner, C. A.; Thornton-Pett, M.; Kennedy, J. D. *Collect. Czech. Chem. Commun.* **2002**, *67*, 869. (d) Jelínek, T.; Thornton-Pett, M.; Kennedy, J. D. *Collect. Czech. Chem. Commun.* **2002**, *67*, 1035. (e) Stíbr, B. *Pure Appl. Chem.* **2003**, *75*, 1295. (f) Brellochs, B.; Backovsky, J.; Stíbr, B.; Jelínek, T.; Holub, J.; Bakardjiev, M.; Hnyk, D.; Hofmann, M.; Císarová, I.; Wrackmeyer, B. *Eur. J. Inorg. Chem.* **2004**, 3605.

(4) Du, S.; Kautz, J. A.; McGrath, T. D.; Stone, F. G. A. *Organometallics* **2003**, *22*, 2842.

(5) (a) Du, S.; Farley, R. D.; Harvey, J. N.; Jeffery, J. C.; Kautz, J. A.; Maher, J. P.; McGrath, T. D.; Murphy, D. M.; Riis-Johannessen, T.; Stone, F. G. A. *Chem. Commun.* **2003**, 1846. (b) Du, S.; Jeffery, J. C.; Kautz, J. A.; Lu, X. L.; McGrath, T. D.; Miller, T. A.; Riis-Johannessen, T.; Stone, F. G. A. *Inorg. Chem.* **2005**, *44*, 2815.

(6) (a) Lei, P.; McGrath, T. D.; Stone, F. G. A. *Chem. Commun.* **2005**, 3706. (b) Lei, P.; McGrath, T. D.; Stone, F. G. A. *Organometallics* **2006**, *25*, 2011.

(7) Lu, X. L.; McGrath, T. D.; Stone, F. G. A. *Organometallics* **2006**, *25*, 2590.

(8) Franken, A.; McGrath, T. D.; Stone, F. G. A. *Inorg. Chem.* **2006**, *45*, 2669.

(9) Franken, A.; McGrath, T. D.; Stone, F. G. A. *Organometallics* **2005**, *24*, 5157.

(10) McGrath, T. D.; Du, S.; Hodson, B. E.; Lu, X. L.; Stone, F. G. A. *Organometallics* **2006**, *25*, 4444.

(11) Du, S.; Kautz, J. A.; McGrath, T. D.; Stone, F. G. A. *Angew. Chem., Int. Ed.* **2003**, *42*, 5728.

10.1021/om060418r CCC: $33.50
Publication on Web 08/17/2006

Chart 1

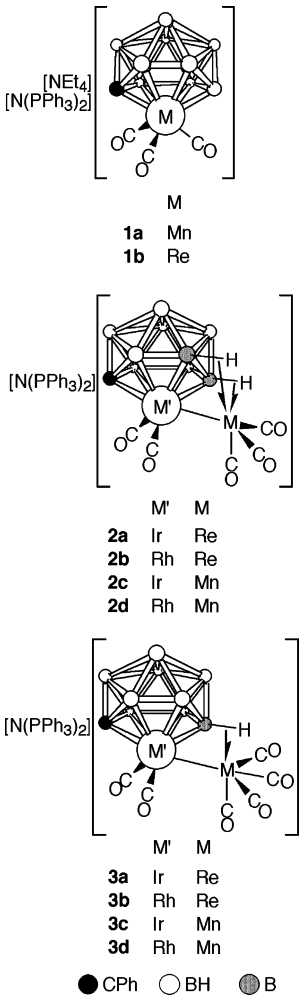

	M
1a	Mn
1b	Re

	M'	M
2a	Ir	Re
2b	Rh	Re
2c	Ir	Mn
2d	Rh	Mn

	M'	M
3a	Ir	Re
3b	Rh	Re
3c	Ir	Mn
3d	Rh	Mn

All of compounds **2**, however, are unstable in solution, and the manganese species **2c** and **2d** are very particularly so. The only observed decomposition products are $[N(PPh_3)_2][1,3\text{-}\{M(CO)_4\}\text{-}3\text{-}(\mu\text{-H})\text{-}1,1\text{-}(CO)_2\text{-}2\text{-Ph-}closo\text{-}1,2\text{-}M'CB_9H_8]$ (M = Re, M′ = Ir (**3a**), Rh (**3b**); M = Mn, M′ = Ir (**3c**), Rh (**3d**)), formed following CO scavenging.[10] Unfortunately, the decomposition process appears to be very significantly accelerated by the presence of impurities—including added reagents—and in consequence we have hitherto been unable to isolate any trimetallic products from reactions of manganese-containing **2c** and **2d** with either $\{Cu(PPh_3)\}^+$ or $\{Au(PPh_3)\}^+$. Although some of **3a** and **3b** are also always obtained in the same reactions with **2a** and **2b**, the substrate Re−Ir and Re−Rh bimetallics are sufficiently stable that they may be converted to heteropolymetallic species, as we now discuss.

Results and Discussion

Reaction of **2a** with the source of $\{Cu(PPh_3)\}^+$ gave the desired heterotrimetallic species, namely, $[1,4,7\text{-}\{Cu(PPh_3)\}\text{-}1,5,6\text{-}\{Re(CO)_3\}\text{-}4,5,6,7\text{-}(\mu\text{-H})_4\text{-}1,1\text{-}(CO)_2\text{-}2\text{-Ph-}closo\text{-}1,2\text{-Ir-}CB_9H_5]$ (**4a**) (see Chart 2). However, formation of the analogous product **4b** from reaction of **2b** with the copper reagent was only transiently observed (deduced from IR and ^{11}B NMR spectroscopy of the reaction mixture). Compound **4b** appears to be formed in extremely low and variable amounts, and its formation is further compromised by significant conversion of **2b** to **3b**. Thus the copper reagent is effectively in excess, a situation that favors the formation of compound **5b** (see below).

Chart 2

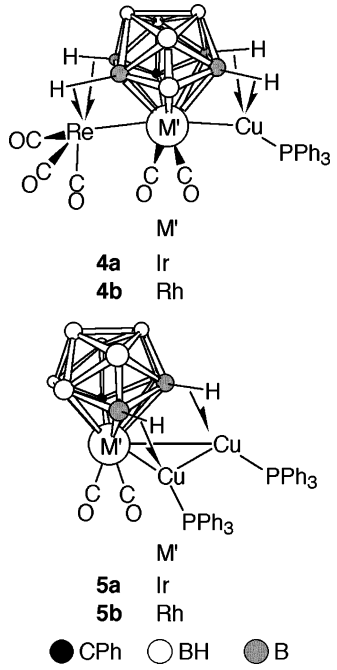

	M'
4a	Ir
4b	Rh

	M'
5a	Ir
5b	Rh

Crystals of **4a** were extremely difficult to obtain, and although one was available for an X-ray diffraction study, it was only of modest quality and weakly diffracting and so an accurate structural determination was not possible. However, a very preliminary experiment (see Supporting Information) did confirm the heavy-atom structure to be that represented by the structure shown in Chart 2. The central iridacarborane core is flanked by $\{Re(CO)_3\}$ and $\{Cu(PPh_3)\}$ moieties, which are attached via Ir−Re and Ir−Cu bonds, respectively; it is additionally deduced that each of these *exo*-polyhedral units is also supported by two agostic-type bridges. Notably, the rhenium fragment has migrated over to a site adjacent to the one occupied in the precursor **2a**. Thus, both *exo*-polyhedral units are now anchored via α- and *β*-BH groups in the C*BB*BBB face that is η^6-bonded to iridium (cf. *β*- and *γ*-BH units for the $\{Re(CO)_3\}$ in **2a**). This is additionally interesting in that it is the only instance of such α-BH coordination that we have observed thus far in these or related {metal−CB_9} systems.

Spectroscopic data for compound **4a** (Tables 1−3) are consistent with an asymmetric solid-state structure and were useful in confirming the proposed architecture. Thus, the $^{11}B\{^1H\}$ NMR spectrum shows nine separate resonances, while the $^{31}P\{^1H\}$ NMR spectrum shows a broad resonance for the copper-bound phosphine at *δ* 9.2. In the ^1H NMR spectrum, two broad, high-field quartet resonances are seen (*δ* −6.73 and −9.18) that are assigned to hydrogens involved in the B−H→Re agostic-type bonds,[12] with no signals attributable to the B−H→Cu units. Peaks are seldom observed for the latter moieties as a result of broadening by the adjacent quadrupolar B and Cu nuclei and by fluxional processes that are rapid on the NMR time scale.[13] The $^{13}C\{^1H\}$ NMR spectrum of **4a** shows as expected five separate signals for the different CO ligands, with the Re-bound groups resonating at *δ* 192.9, 192.5, and 189.4 and those bound to Ir at *δ* 176.4 and 168.0.

(12) Brew, S. A.; Stone, F. G. A. *Adv. Organomet. Chem.* **1993**, *35*, 135.
(13) (a) Jeffrey, J. C.; Ruiz, M. A.; Sherwood, P.; Stone, F. G. A. *J. Chem. Soc., Dalton Trans.* **1989**, 1845. (b) Carr, N.; Gimeno, M. C.; Goldberg, J. E.; Pilotti, M. U.; Stone, F. G. A.; Topaloglu, I. *J. Chem. Soc., Dalton Trans.* **1990**, 2253. (c) Jeffery, J. C.; Jelliss, P. A.; Stone, F. G. A. *J. Chem. Soc., Dalton Trans.* **1993**, 1073. (d) Jeffery, J. C.; Jelliss, P. A.; Rees, L. H.; Stone, F. G. A. *Organometallics* **1998**, *17*, 2258.

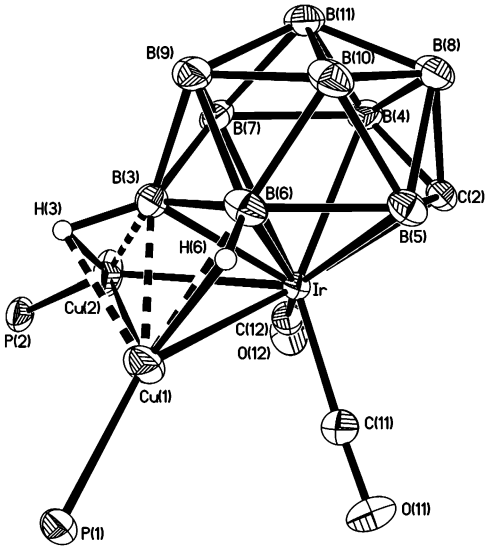

Figure 1. Structure of **5a** showing the crystallographic labeling scheme. In this and subsequent figures, thermal ellipsoids are shown with 40% probability and for clarity only chemically significant H atoms are shown and phenyl rings are omitted. Selected distances (Å) and angles (deg) are as follows: Ir−Cu(1) 2.6799(3), Ir−Cu(2) 2.6047(3), Ir−C(2) 2.1525(18), Ir−B(3) 2.246(2), Ir−B(4) 2.420(2), Ir−B(5) 2.395(2), Ir−B(6) 2.427(2), Ir−B(7) 2.394(2), B(3)···Cu(1) 2.137(2), B(3)···Cu(2) 2.084(2), B(6)···Cu(1) 2.223(2), B(7)···Cu(2) 2.564(3), Cu(1)−Cu(2) 2.9051(5); Cu(2)−Ir−Cu(1) 66.678(11), Ir−Cu(1)−Cu(2) 55.421(8), Ir−Cu(2)−Cu(1) 57.901(9).

In addition to compound **4a**, reaction of **2a** with $\{Cu(PPh_3)\}^+$ also gave another type of trimetallic product; a similar species was obtained from **2b** and the same copper reagent. These were the dicopper complexes [1,3,6-$\{Cu_2(PPh_3)_2\}$-3,6-(μ-H)$_2$-1,1-(CO)$_2$-2-Ph-*closo*-1,2-M′CB_9H_7] (M′ = Ir (**5a**), Rh (**5b**)) (see Chart 2), which were identified by an X-ray diffraction study on **5a**. The structure so obtained is shown in Figure 1. As can be seen, the iridacarborane core supports a dicopper unit, so that overall an $\{IrCu_2\}$ metal triangle is present (Ir−Cu(1) = 2.6799(3), Ir−Cu(2) = 2.6047(3), Cu(1)−Cu(2) = 2.9051(5) Å). The structure of this trimetallic assembly contrasts with the V-shaped unit in compound **4a** and that in the previously reported dicopper derivative of **1b**.[4]

The NMR data for compounds **5** (Tables 2 and 3) are at odds with the structure determined crystallographically, as they appear to show mirror symmetry in solution. A 1:1:1:2:2:2 pattern of intensities is seen (with one coincidence for **5b**) in their $^{11}B\{^1H\}$ spectra, while their $^{31}P\{^1H\}$ spectra show only a single broad resonance at δ 9.2 (**5a**) and 9.5 (**5b**). This would be consistent with time-averaged symmetry and suggests that the copper fragments are fluxional over the surface of the metallacarborane core.[13] Such processes might involve breaking of the Cu−Cu connectivity to give an intermediate with a V-shaped trimetal unit (cf. compounds **4**) or else a migration of the entire $\{Cu_2(PPh_3)_2\}$ unit. As with **4**, however, these mechanisms are rapid on the NMR time scale, even at low temperature:[13] they could not be arrested upon cooling, and so two separate ^{31}P resonances were not obtained. Such processes also preclude the observation of signals for the B−H⇀Cu units in the ^1H NMR spectrum as noted for **4**.

In contrast with the reactions of **2a** and **2b** with the $\{Cu(PPh_3)\}^+$ fragment, reactions of the same metallacarboranes with a source of $\{Au(PPh_3)\}^+$ proceed somewhat differently, and up to four polymetallic products may be formed. With **2a** and the gold reagent, no evidence was seen of an "expected" heterotrimetallic Re−Ir−Au species that could have a structure related to that of compound **4a**. However, from **2b** and $\{Au(PPh_3)\}^+$ a product **6b**, initially presumed structurally analogous to **4b**, was obtained.

Characterizing data for compound **6b** are given in Tables 1−3. From the ^1H NMR spectrum, it was evident that only a single phosphine unit was present and, as for **4a**, there are two broad quartet resonances for B−H⇀Re linkages, at δ −6.32 and −7.14, but no peaks for B−H⇀Au groups. The $^{13}C\{^1H\}$ NMR spectrum confirmed the presence of five different CO ligands, with the three Re-bound groups resonating at δ 193.6, 192.8, and 187.8, while the Rh−CO units appear as doublets at δ 185.4 and 179.9 (J(RhC) = 71 and 70 Hz, respectively). Similarly, the $^{11}B\{^1H\}$ NMR spectrum also suggests an asymmetric structure, with peaks in the ratio 1:2:1:2:1:1:1, while the single gold-bound PPh_3 ligand resonates at δ 50.9 in the $^{31}P\{^1H\}$ NMR spectrum.

All of the above data suggested that **6b** had a structure closely related to that of **4a**, as might be expected. Nevertheless, an X-ray diffraction study on the gold species was merited for confirmation of this, particularly as the gold center was anticipated not to show the pseudo-tetrahedral coordination seen for copper in **4a**. This experiment, however, revealed complex **6b** to have the molecular structure shown in Figure 2, and the compound is, in fact, [8,9,10-*endo*-$\{Au(PPh_3)\}$-3,4,8-*exo*-$\{Re(CO)_3\}$-3,4-(μ-H)$_2$-8,8-(CO)$_2$-7-Ph-*nido*-8,7-$RhCB_9H_7$] (see also Scheme 1). The $\{RhCB_9\}$ core of this species clearly has a *nido*-11-vertex structure, with the $\{Re(CO)_3\}$ fragment in an *exo*-polyhedral site, as expected, but with the $\{Au(PPh_3)\}$ moiety occupying a site that is *endo*-polyhedral with respect to the open RhCBBB face of the {*nido*-8,7-$RhCB_9$} cluster. The rhenium center is attached to the cage via an Rh−Re bond (Rh(1)−Re(1) = 2.8333(8) Å) and two B−H⇀Re agostic-type interactions that involve B(3) and B(4) in the upper pentagonal B_5 belt (Re(1)···B(3) = 2.383(8), Re(1)−H(3) = 2.05(7), Re(1)···B(4) = 2.372(8), Re(1)−H(4) = 1.87(7) Å). In contrast, the gold unit is approximately η^3-bound to three atoms in the RhCBBB ring: there is a bond to the rhodium vertex (Rh(1)−Au(1) = 2.8206(7) Å) and two adjacent boron atoms (Au(1)−B(9) = 2.439(9), Au(1)−B(10) = 2.222(10) Å). This bonding for the gold fragment is reminiscent of that in several other, simpler gold complexes of *nido*-11-vertex carboranes.[14−17]

On the basis of electron-counting rules[18−20] and by analogy with other compounds presented herein, the $\{(CO)_2RhCB_9H_9Ph\}^{2-}$ cluster of **6b** would be expected to have a *closo* structure, and thus its observed *nido* character was surprising. However, there are a large number of precedents for 11-vertex metallaheteroboranes of the later transition metals having *nido* structures despite a formal *closo* electron count, examples of which include the $\{L_2PtB_{10}\}$, $\{L_2RhC_2B_8\}$, and $\{L_2RhSB_9\}$ systems.[21−24] Indeed, among the rhodathiaborane species [8,8-L_2-*nido*-8,7-$RhSB_9H_{10}$] it has been shown that these compounds

(14) Hamilton, E. J. M.; Welch, A. J. *Polyhedron* **1990**, *9*, 2407.
(15) Hamilton, E. J. M.; Welch, A. J. *Acta Crystallogr.* **1990**, *C46*, 1228.
(16) Jeffery, J. C.; Jelliss, P. A.; Stone, F. G. A. *Inorg. Chem.* **1993**, *32*, 3382.
(17) Jeffery, J. C.; Jelliss, P. A.; Stone, F. G. A. *J. Chem. Soc., Dalton Trans.* **1993**, 1073.
(18) Wade, K. *Adv. Inorg. Chem. Radiochem.* **1976**, *18*, 1.
(19) Williams, R. E. *Adv. Inorg. Chem. Radiochem.* **1976**, *18*, 67.
(20) Mingos, D. M. P. *Acc. Chem. Res.* **1984**, *17*, 311.
(21) Boocock, S. K.; Greenwood, N. N.; Kennedy, J. D.; McDonald, W. S.; Staves, J. *J. Chem. Soc., Dalton Trans.* **1981**, 2573.
(22) Lu, P.; Knobler, C. B.; Hawthorne, M. F. *Acta Crystallogr.* **1984**, *C40*, 1704.

Table 1. Analytical and Physical Data

compd	color	yield/%[a]	ν_{max}(CO)[b]/cm^{-1}	anal.[c] (%) C	anal.[c] (%) H
[1,4,7-{Cu(PPh$_3$)}-1,5,6-{Re(CO)$_3$}-4,5,6,7-(μ-H)$_4$-1,1-(CO)$_2$-2-Ph-*closo*-1,2-IrCB$_9$H$_5$] (**4a**)	pale yellow	12	2067 s, 2035 s, 2019 s, 1944 br s	37.4 (37.8)[d]	3.5 (3.7)
[1,3,6-{Cu$_2$(PPh$_3$)$_2$}-3,6-(μ-H)$_2$-1,1-(CO)$_2$-2-Ph-*closo*-1,2-IrCB$_9$H$_7$] (**5a**)	yellow	41	2023 s, 1974 s	48.2 (48.0)[e]	4.1 (4.0)
[1,3,6-{Cu$_2$(PPh$_3$)$_2$}-3,6-(μ-H)$_2$-1,1-(CO)$_2$-2-Ph-*closo*-1,2-RhCB$_9$H$_7$] (**5b**)	orange	22	2021 s, 1960 s	48.3 (48.0)[f]	3.9 (4.1)
[8,9,10-*endo*-{Au(PPh$_3$)}-3,4,8-*exo*-{Re(CO)$_3$}-3,4-(μ-H)$_2$-8,8-(CO)$_2$-7-Ph-*nido*-8,7-RhCB$_9$H$_7$] (**6b**)	red-orange	9	2087 s, 2048 s, 2038 vs, 1943 br vs	33.0 (33.2)	2.7 (2.7)
[1,6-{Au$_2$(PPh$_3$)$_2$}-6-(μ-H)-1,1-(CO)$_2$-2-Ph-*closo*-1,2-IrCB$_9$H$_8$] (**7a**)	yellow	39	2044 s, 2000 s	39.1 (38.9)[e]	3.2 (3.2)
[1,6-{Au$_2$(PPh$_3$)$_2$}-6-(μ-H)-1,1-(CO)$_2$-2-Ph-*closo*-1,2-RhCB$_9$H$_8$] (**7b**)	orange	7	2053 s, 2011 s	41.6 (41.6)[e]	2.9 (3.4)
[1,3,6-{Au$_2$(PPh$_3$)$_2$Re(CO)$_3$}-6-(μ-H)-1,1-(CO)$_2$-2-Ph-*closo*-1,2-IrCB$_9$H$_7$] (**8a**)	orange	16	2051 s, 2009 vs, 1929 s, 1915 br s	35.1 (35.3)	2.7 (2.7)
[1,3,6-{Au$_2$(PPh$_3$)$_2$Re(CO)$_3$}-6-(μ-H)-1,1-(CO)$_2$-2-Ph-*closo*-1,2-RhCB$_9$H$_7$] (**8b**)	red	7	2058 s, 2013 vs, 1927 s, 1918 br s	36.2 (36.2)[g]	2.8 (2.8)
[1,3-{Au$_3$(PPh$_3$)$_3$}-1,1-(CO)$_2$-2-Ph-*closo*-1,2-IrCB$_9$H$_8$] (**9a**)	yellow	13	2017 s, 1969 s	40.3 (40.3)[g]	3.2 (3.2)
[1,3-{Au$_3$(PPh$_3$)$_3$}-1,1-(CO)$_2$-2-Ph-*closo*-1,2-RhCB$_9$H$_8$] (**9b**)	yellow	5	2027 s, 1983 s	42.9 (43.0)[e]	3.4 (3.4)

[a] Yields based on available **2a** or **2b** (see text). [b] Measured in CH_2Cl_2; in addition, the spectra of all compounds show a broad, medium-intensity band ca. 2500−2550 cm^{-1} due to B−H absorptions. [c] Calculated values are given in parentheses. [d] Cocrystallized with 1.0 molar equiv of C_5H_{12}. [e] Cocrystallized with 0.5 molar equiv of CH_2Cl_2. [f] Cocrystallized with 2.0 molar equiv of CH_2Cl_2. [g] Cocrystallized with 1.0 molar equiv of CH_2Cl_2.

Table 2. ^{1}H and ^{13}C NMR Data[a]

compd	^{1}H/δ [b]	^{13}C/δ[c]
4a	7.59−7.48 (m, 17H, PPh and cage-C$_6H_5$),[d] 7.26 (m, 2H, cage-C$_6H_5$), 7.22 (m, 1H, cage-C$_6H_5$), −6.73 (br q, J(BH) ≈ 100, 1H, B−H⇀Re), −9.18 (br q, J(BH) ≈ 110, 1H, B−H⇀Re)	192.9, 192.5, 189.4 (Re−CO), 176.4, 168.0 (Ir−CO), 145.1, 134.1−128.9 (Ph), 47.8 (br, cage C)
5a	7.84 (m, 2H, cage-C$_6H_5$),[d] 7.45−7.12 (m, 33H, PPh and cage-C$_6H_5$)	172.3 (CO), 149.1, 134.1−126.0 (Ph), 63.5 (br, cage C)
5b	7.84 (m, 2H, cage-C$_6H_5$),[d] 7.51−7.33 (m, 30H, PPh), 7.27 (m, 2H, cage-C$_6H_5$), 7.15 (m, 1H, cage-C$_6H_5$)	186.7 (br, CO), 149.3, 135.0−126.1 (Ph), 59.3 (br, cage C)
6b	7.62−7.51 (m, 16H, PPh and cage-C$_6H_5$), 7.45 (m, 2H, cage-C$_6H_5$), 7.17 (m, 2H, cage-C$_6H_5$), −6.32 (br q, J(BH) ≈ 100, 1H, B−H⇀Re), −7.14 (vbr q, J(BH) ≈ 100, 1H, B−H⇀Re)	193.6, 192.8, 187.8 (Re−CO), 185.4 (d, J(RhC) = 71, Rh−CO), 179.9 (d, J(RhC) = 70, Rh−CO), 149.4, 134.6−126.7 (Ph), 61.0 (br, cage C)
7a	7.93 (m, 2H, cage-C$_6H_5$),[d] 7.56−6.99 (m, 33H, PPh and cage-C$_6H_5$)	172.8 (CO), 148.4, 136.4−126.4 (Ph), 54.2 (br, cage C)
7b	7.84 (m, 2H, cage-C$_6H_5$),[d] 7.46−7.33 (m, 30H, PPh), 7.20 (m, 1H, cage-C$_6H_5$), 7.10 (m, 2H, cage-C$_6H_5$)	191.5 (d, J(RhC) = 60, CO), 149.8, 134.6−126.2 (Ph), 74.5 (br, cage C)
8a	7.87 (m, 2H, cage-C$_6H_5$), 7.49−7.16 (m, 33H, PPh and cage-C$_6H_5$), ca. −8.9 (vbr, 1H, B−H⇀Re)	198.0, 194.8, 192.6 (br × 3, Re−CO), 175.4, 171.0 (Ir−CO), 147.2, 135.4−126.8 (Ph), 56.1 (br, cage C)
8b	7.88 (m, 2H, cage-C$_6H_5$), 7.48−7.18 (m, 33H, PPh and cage-C$_6H_5$), ca. −7.9 (vbr, 1H, B−H⇀Re)	197.1, 192.8, 190.4 (br × 3, Re−CO), 185.7, 182.2 (br × 2, Rh−CO), 147.7, 134.4−126.7 (Ph), 49.3 (br, cage C)
9a	7.83 (m, 2H, cage-C$_6H_5$), 7.45−7.07 (m, 48H, PPh and cage-C$_6H_5$)	177.2 (CO), 150.4, 134.4−125.4 (Ph), 73.2 (br, cage C)
9b	7.79 (m, 2H, cage-C$_6H_5$), 7.58−7.06 (m, 48H, PPh and cage-C$_6H_5$)	182.5 (d, J(RhC) = 54, CO), 149.7, 134.6−125.3 (Ph), 67.7 (br, cage C)[e]

[a] Chemical shifts (δ) in ppm, coupling constants (J) in hertz, measurements at ambient temperatures, except where indicated, in CD_2Cl_2. [b] Resonances for terminal BH protons occur as broad unresolved signals in the range δ ca. −1 to +3. [c] ^{1}H-decoupled chemical shifts are positive to high frequency of $SiMe_4$. [d] Signals for B−*H*⇀M″ protons (M″ = Cu, Au) are not observed. [e] Tentative assignment.

reversibly undergo cage-closure reactions upon deprotonation.[25] Similarly, closed-cage species are also found where the proton is otherwise absent due to the presence instead of a boron-bound two-electron-donor substituent.[26] The proton so eliminated in both types of complex occupied a bridging position in the open face of the rhodathiaborane cluster, akin to the {Au(PPh$_3$)}$^+$ fragment in **6b**: the gold−phosphine moiety is isolobal with the proton,[27] and hence a close parallel can be drawn between the present case and the earlier rhodathiaboranes. In this respect, the structure of compound **6b** may also be compared with that of [10,11-*endo*-{Au(PPh$_3$)}-9-(η-C$_5$H$_5$)-*nido*-9,7,8-NiC$_2$B$_8$H$_{10}$], where the {Au(PPh$_3$)} moiety also occupies an *endo* site over the open face of an 11-vertex metallacarborane and of which the {NiC$_2$B$_8$} core should also be closed (in electron-counting terms) but has a *nido* structure.[28] In the nickel system, however, there is no Ni−Au bond (Ni···Au > 3 Å), contrasting with the Rh−Au connectivity present in compound **6b**.

In addition to the "expected" trimetallic product exemplified by **6b**, the reactions of **2a** and **2b** with {Au(PPh$_3$)}$^+$ each also

(23) (a) Ferguson, G.; Jennings, M. C.; Lough, A. J.; Coughlan, S.; Spalding, T. R.; Kennedy, J. D.; Fontaine, X. L. R.; Stíbr, B. *J. Chem. Soc., Chem. Commun.* **1990**, 891. (b) Adams, K. J.; McGrath, T. D.; Welch, A. J. *Acta Crystallogr.* **1995**, *C51*, 401. (c) Macías, R.; Rath, N. P.; Barton, L. *Organometallics* **1999**, *18*, 3637.

(24) See also: Kennedy, J. D. In *The Borane, Carborane, Carbocation Continuum*; Casanova, J., Ed.; Wiley: New York, 1998; p 85.

(25) Adams, K. J.; McGrath, T. D.; Thomas, Rh. Ll.; Weller, A. S.; Welch, A. J. *J. Organomet. Chem.* **1997**, *527*, 283.

(26) (a) Coughlan, S.; Spalding, T. R.; Ferguson, G.; Gallagher, J. F.; Lough, A. J.; Fontaine, X. L. R.; Kennedy, J. D.; Stíbr, B. *J. Chem. Soc., Dalton Trans.* **1992**, 2865. (b) Volkov, O.; Macías, R.; Rath, N. P.; Barton, L. *J. Organomet. Chem.* **2002**, *657*, 40.

(27) (a) Hoffmann, R. *Angew. Chem., Int. Ed. Engl.* **1982**, *21*, 711. (b) Stone, F. G. A. *Angew. Chem., Int. Ed. Engl.* **1984**, *23*, 89.

(28) Barker, G. K.; Godfrey, N. R.; Green, M.; Parge, H. E.; Stone, F. G. A.; Welch, A. J. *J. Chem. Soc., Chem. Commun.* **1983**, 277.

Table 3. ^{11}B and ^{31}P NMR Data[a]

compd	^{11}B/δ [b]	^{31}P/δ [c]
4a	38.4 (br), 6.9, 2.9, −9.4 (br), −13.9, −16.8 (br), −22.5, −23.7, −32.0	9.2 (br)
5a	7.6, ca. 6.3 (vbr), −7.1, −10.4 (br, 2B), −28.8 (2B), −31.3 (2B)	9.2 (br)
5b	7.2 (2B), 2.8, −9.3 (2B), −26.5 (2B), −30.9 (2B)	9.5 (br)
6b	19.1 (br), 2.9 (2B), −6.6, −8.3 (2B), −10.8, −12.8, −15.7	50.9
7a	11.1, 9.2 (br), 0.5, −5.2 (br, 2B), −27.6 (4B)	44.7
7b	11.3, 7.4, 2.0, −3.5 (br, 2B), −18.0 (2B), −22.1 (2B)	40.0
8a	37.9 (B(3)), 18.3, 8.6 (br), −5.6 (vbr), −10.2 (br), −18.8 (br), −21.2 (2B), −33.6	58.7 (br), 51.1 (br)
8b	46.9 (B(3)), 20.4, 9.1 (br), −1.1 (vbr), −5.2 (vbr), −11.1, −13.1, −17.5, −30.2	56.3 (br), 48.6 (br)
9a	21.3 (B(3)), 9.2, ca. 7.5 (br, sh), −9.4 (br, 2B), −23.6 (2B), −30.0 (2B)	43.6 (br)
9b	27.3 (B(3)), 9.1 (2B), −5.8 (br, 2B), −15.6 (2B), −24.5 (2B)	40.8 (br)

[a] Chemical shifts (δ) in ppm, coupling constants (J) in hertz, measurements at ambient temperatures in CD_2Cl_2. [b] ^{1}H-decoupled chemical shifts are positive to high frequency of $BF_3{\cdot}Et_2O$ (external); resonances are of unit integral except where indicated, and where peaks are broad the assigned integrals are somewhat subjective. [c] ^{1}H-decoupled chemical shifts are positive to high frequency of 85% H_3PO_4 (external).

gave digold products, namely, [1,6-{$Au_2(PPh_3)_2$}-6-(μ-H)-1,1-$(CO)_2$-2-Ph-*closo*-1,2-M′CB_9H_8] (M′ = Ir (**7a**), Rh (**7b**)) (see Scheme 1), which are akin to compounds **5**. Spectroscopic data for compounds **7** are listed in Tables 1−3. In their IR spectra, only two CO bands are seen, consistent with loss of the *exo*-polyhedral {$Re(CO)_3$} fragment. Similarly, the ^{1}H and ^{13}C{^{1}H} NMR spectra are straightforward, showing only peaks for the carborane and PPh_3 groups (in the ratio 1:2) and only a single

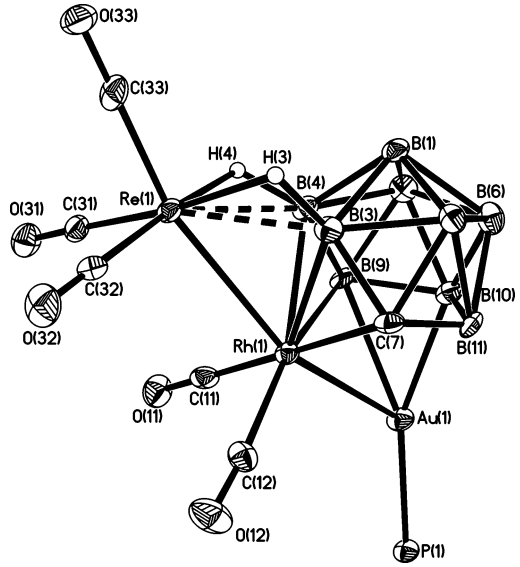

Figure 2. Structure of compound **6b** showing the crystallographic labeling scheme. Selected internuclear distances (Å) and interbond angles (deg) are as follows: Rh(1)−Au(1) 2.8206(7), Rh(1)−Re(1) 2.8333(8), Rh(1)−B(3) 2.295(9), Rh(1)−B(4) 2.275(9), Rh(1)−C(7) 2.188(7), Rh(1)−B(9) 2.287(8), Re(1)···B(3) 2.383(8), Re(1)···B(4) 2.372(8), Au(1)−B(9) 2.439(9), Au(1)−B(10) 2.222(10); Au(1)−Rh(1)−Re(1) 150.08(2).

resonance for CO ligands (δ 172.8 (**7a**), 191.5 (**7b**; d, J(RhC) = 60 Hz)). Similar to compounds **5**, the ^{11}B{^{1}H} NMR spectra of compounds **7** indicate mirror symmetry in solution, with both having peaks in 1:1:1:2:2:2 intensity ratios (**7a** has one coincidence); likewise, only a single ^{31}P{^{1}H} NMR signal (δ 44.7 (**7a**), 40.0 (**7b**)) is evident. This is again attributable to

Scheme 1. Possible Sequence of Formation of Gold−Phosphine Derivatives from Compounds 2a and 2b

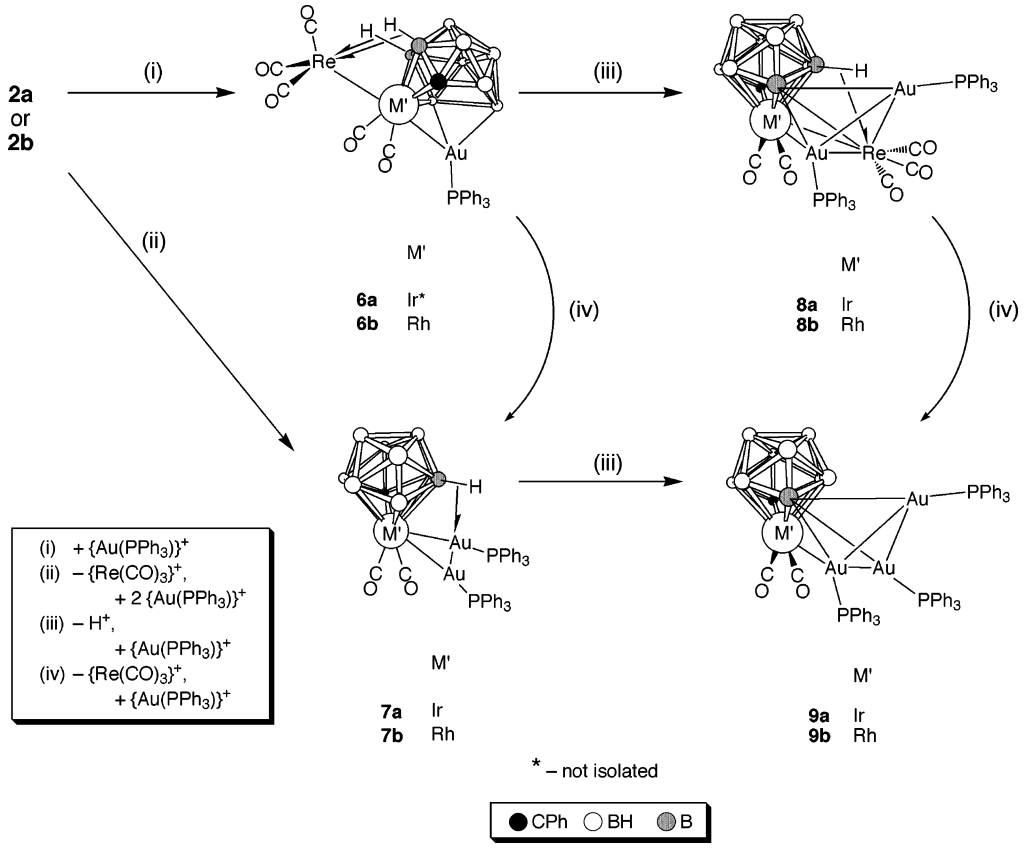

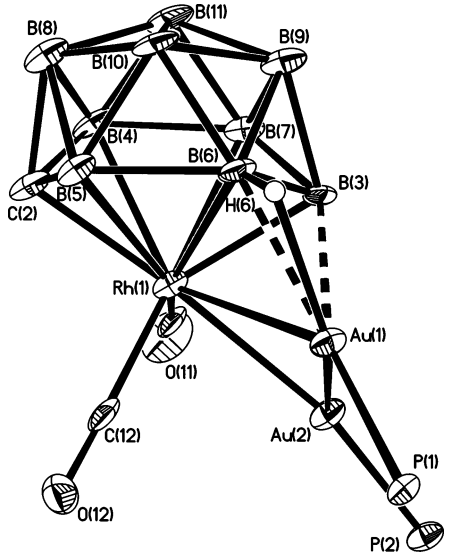

Figure 3. Structure of compound **7b** showing the crystallographic labeling scheme. Selected internuclear distances (Å) and interbond angles (deg) are as follows: Rh(1)−C(2) 2.173(10), Rh(1)−B(3) 2.237(12), Rh(1)−B(4) 2.452(12), Rh(1)−B(5) 2.476(12), Rh(1)−B(6) 2.467(12), Rh(1)−B(7) 2.334(12), Rh(1)−Au(1) 2.9723(9), Rh(1)−Au(2) 2.6635(9), Au(1)−Au(2) 2.8335(6), Au(1)−H(6) 1.98(9), B(6)···Au(1) 2.298(11), B(3)···Au(1) 2.455(12), B(3)···Au(2) 2.945(12), C(11)···Au(2) 2.701(10); Au(2)−Rh(1)−Au(1) 60.07(2), Au(2)−Au(1)−Rh(1) 54.552(19), Rh(1)−Au(2)−Au(1) 65.38(2).

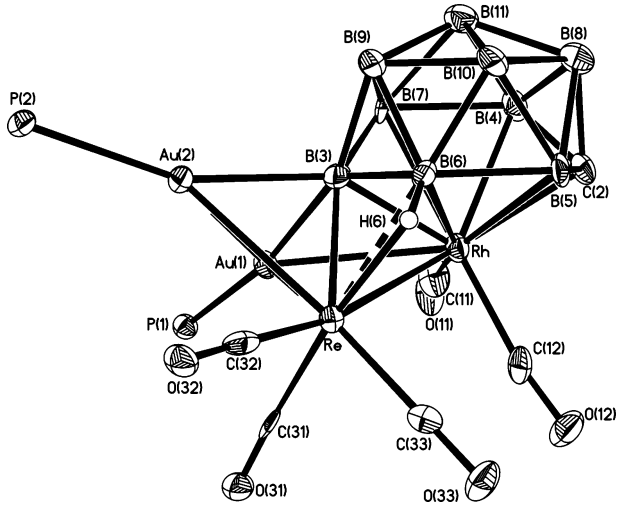

Figure 4. Structure of **8b** showing the crystallographic labeling scheme. Selected distances (Å) and angles (deg) are as follows: Rh−C(2) 2.154(7), Rh−B(3) 2.206(9), Rh−B(4) 2.372(9), Rh−B(5) 2.440(9), Rh−B(6) 2.344(9), Rh−B(7) 2.351(9), Rh−Au(1) 2.9106(7), Rh−Re 2.9581(7), B(3)−Au(1) 2.229(8), B(3)−Au(2) 2.301(9), B(3)···Re 2.336(9), B(6)···Re 2.329(8), Re−Au(2) 2.8619(5), Re−Au(1) 2.9983(5), Au(1)−Au(2) 2.7859(4); Au(1)−Rh−Re 61.439(16), Au(2)−Re−Rh 96.883(17), Au(2)−Re−Au(1) 56.713(12), Rh−Re−Au(1) 58.499(15), Au(2)−Au(1)−Rh 99.718(17), Au(2)−Au(1)−Re 59.176(11), Rh−Au(1)−Re 60.061(15), Au(1)−Au(2)−Re 64.111(12).

migration of the *exo*-polyhedral moieties to give a structure with time-averaged symmetry, as discussed above.

For comparison with compounds **5**, and to definitively confirm the architecture of compounds **7**, an X-ray diffraction study was undertaken on **7b**, revealing the structure shown in Figure 3. As expected, the molecule of **7b** is similar to compounds **5**, in that it consists of a central {*closo*-1,2-$RhCB_9$} core, of which the Rh vertex and two *exo*-polyhedral {$Au(PPh_3)$} units are involved in an {$RhAu_2$} triangle (Rh(1)−Au(1) 2.9723(9), Rh(1)−Au(2) 2.6635(9), Au(1)−Au(2) 2.8335(6) Å). The molecule is asymmetric, and this feature, like the structure of **5a**, contrasts with the symmetry implied by solution NMR spectra. One of the gold atoms (Au(1)) is also involved in an agostic-type linkage with BH(6) (Au(1)···B(6) = 2.298(11) Å) and a much longer interaction with BH(3) (Au(1)···B(3) = 2.455(12) Å). However, the second gold center (Au(2)) is not supported by any B−H⇀Au interactions, but instead enjoys only the two metal−metal bonds and a very long interaction with one of the rhodium-bound carbonyl ligands (Au(2)···C(11) = 2.701(10) Å). Thus, the structure of compounds **7** is somewhat different from that of compounds **5**, where the copper centers can be considered more intimately bonded to the cage. This can be attributed to the known preference of gold for a lower coordination number than copper.[29]

In addition to compounds **6** and **7**, a third type of polymetallacarborane species of a novel structural class was isolated from interaction of **2a** or **2b** with the $\{Au(PPh_3)\}^+$ source: these species, compounds **8**, are certainly the most interesting of the products obtained. Initial spectroscopic analysis (Tables 1−3) indicated the presence of Re and Au fragments in addition to the irida- or rhoda-carborane core, and, significantly, both ^{31}P and ^{1}H NMR data suggested there were *two* {$Au(PPh_3)$} moieties present. The nature of compounds **8** was ultimately determined by X-ray diffraction studies,[11] of which the structure of the rhodium derivative **8b** is shown in Figure 4.

Compounds **8** are the tetrametallic species [1,3,6-{$Au_2(PPh_3)_2$-$Re(CO)_3$}-6-(μ-H)-1,1-$(CO)_2$-2-Ph-*closo*-1,2-M′CB_9H_7] (M′ = Ir (**8a**), Rh (**8b**)), in which {$Re(CO)_3$} and {$Au(PPh_3)$} moieties are bonded to the cluster {M′$(CO)_2$} vertex and to each other. In addition, the Re−Au vector is bridged by a second {$Au(PPh_3)$} fragment, so that overall an {M′Au_2Re} "butterfly" has been assembled, starting from the rhenacarborane of **1b**. Distances within this "butterfly" in **8b** are Rh−Re = 2.9581(7), Rh−Au(1) = 2.9106(7), Re−Au(1) = 2.9983(5), Re−Au(2) = 2.8619(5), and Au(1)−Au(2) = 2.7859(4) Å. The *exo*-polyhedral rhenium center is additionally supported by a B−H⇀Re agostic-type linkage (B(6)−Re = 2.329(8), Re−H(6) = 1.93(6) Å) that involves a β-BH vertex in the Rh-bound CB*B*BBB belt. Notably, the adjacent γ-boron atom in this CBB*B*BB belt lacks a terminal hydrogen atom and moreover is in contact with all four of the metal atoms (B(3)−Rh = 2.206(9), B(3)−Au(1) = 2.229(8), B(3)−Au(2) = 2.301(9), B(3)−Re = 2.336(9) Å). As a result, the coordination around this boron atom in the trigonal bipyramidal {BM′Au_2Re} core resembles that in transition metal boride clusters.[30]

The NMR spectra for compounds **8** (Tables 2 and 3) are entirely consistent with the solid-state structure. Specifically, their $^{11}B\{^1H\}$ NMR spectra shown nine separate resonances (with one coincidence for **8a**), as required by the lack of molecular symmetry. The resonance for B(3), which lacks a terminal hydrogen and is in contact with all four metal centers, remains a singlet in the fully proton-coupled spectrum and occurs at δ 37.9 for **8a** and δ 46.9 for **8b**. Despite the metal boride structural analogy that was drawn above, the chemical shift of this boron atom in compounds **8**—although it is rather

(29) See, for example: Carvajal, M. A.; Novoa, J. J.; Alvarez, S. *J. Am. Chem. Soc.* **2004**, *126*, 1465.

(30) Housecroft, C. E. *Coord. Chem. Rev.* **1995**, *143*, 297.

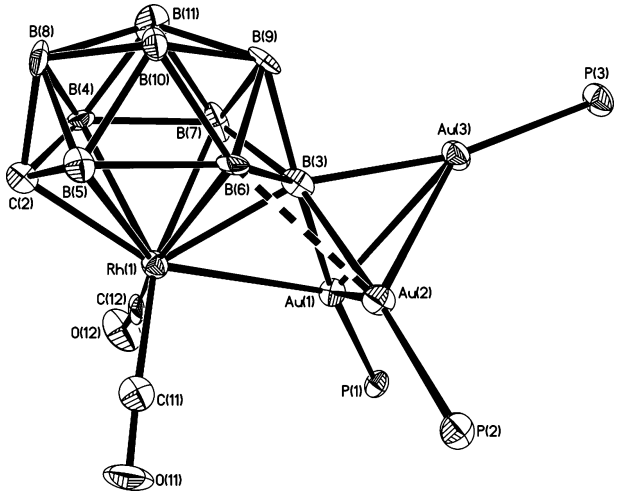

Figure 5. Structure of compound **9b** showing the crystallographic labeling scheme. Selected distances and angles are as follows: Au(1)−Au(2) 2.8693(5), Au(2)−Au(3) 2.8046(5), Au(1)−Au(3) 2.8025(6), Au(1)−Rh(1) 2.8145(9), Au(1)−B(3) 2.230(12), Au(2)−B(3) 2.253(11), Au(3)−B(3) 2.247(11), Au(2)···B(6) 2.548(12), Rh(1)−C(2) 2.150(10), Rh(1)−B(3) 2.245(10), Rh(1)−B(4) 2.363(11), Rh(1)−B(5) 2.408(12), Rh(1)−B(6) 2.438(11), Rh(1)−B(7) 2.320(11); Au(2)−Au(1)−Au(3) 59.259(13), Au(1)−Au(2)−Au(3) 59.185(14), Au(1)−Au(3)−Au(2) 61.556(14), Au(3)−Au(1)−Rh(1) 102.74(2), Au(2)−Au(1)−Rh(1) 72.195(19).

downfield—is definitely more typical of a metallacarborane[12] than a boride, where the boron atom experiences much greater deshielding (typically, $\delta \approx 100-200$).[30] In their $^{31}P\{^1H\}$ NMR spectra, compounds **8** each show two separate, broad resonances for the two different $\{Au(PPh_3)\}$ units, at δ 58.7 and 51.1 for **8a** and δ 56.3 and 48.6 for **8b**. Likewise, their ^1H and $^{13}C\{^1H\}$ NMR spectra show all the expected features: in particular five different CO resonances and a single very broad, high-field proton resonance (δ ca. −8.9 (**8a**) and −7.9 (**8b**)) for the sole B−H→Re linkage in each molecule.

The fourth product type obtained from reaction of **2a** or **2b** with the $\{Au(PPh_3)\}^+$ fragment is related to the above compounds **8**. These species are the trigold-irida- or -rhodacarborane complexes [1,3-$\{Au_3(PPh_3)_3\}$-1,1-$(CO)_2$-2-Ph-*closo*-1,2-M′CB_9H_8] (M′ = Ir (**9a**), Rh (**9b**)), which are typically isolated only in very small quantities and only when the reaction time is a day or more. This is hardly surprising, as the stoichiometry of the reaction (the ratio of **2a** or **2b** to Au is 1:1) strongly disfavors their formation. However, compounds **9** are obtained in larger quantities when the above reactant stoichiometry is 1:2 or when CH_2Cl_2 solutions of compounds **7** are allowed to decompose over several days; the former method is, of course, the more satisfactory. Treatment of compounds **7** with further $\{Au(PPh_3)\}^+$ also affords compounds **9**: we note that this is analogous to the observation that **8b** is formed from **6b** under similar conditions. Compounds **9** were initially identified via an X-ray diffraction experiment on **9b**, of which the results are shown in Figure 5. The structure of **9a** has also been determined and is essentially identical to that of **9b**, and is included as electronic Supporting Information only.

The molecule of **9b** consists of a central {*closo*-1,2-$RhCB_9$} core, to which is bonded a triangular $\{Au_3(PPh_3)_3\}$ unit (Au(1)−Au(2) 2.8693(5), Au(1)−Au(3) 2.8025(6), Au(2)−Au(3) 2.8046(5) Å). One of the gold centers is directly bonded to the cluster rhodium vertex (Au(1)−Rh(1) = 2.8145(9) Å) and all three of the gold atoms are in contact with B(3) (Au(1)−B(3) 2.230(12), Au(2)−B(3) 2.253(11), Au(3)−B(3) 2.247(11) Å), similar to the situation in compounds **8**: this boron vertex likewise lacks a terminal hydrogen atom. However, although this boron atom is also directly bonded to the fourth metal atom, namely, the rhodium vertex (Rh(1)−B(3) = 2.245(10) Å), there is no connectivity between Rh(1) and Au(2) (Rh(1)···Au(2) is >3.3 Å), and this eliminates a closer similarity to compounds **8**.

Spectroscopic data for compounds **9** are listed in Tables 1−3. These bear some similarity to those for compounds **7**, with both $^{11}B\{^1H\}$ and $^{31}P\{^1H\}$ NMR spectra also indicating a symmetric structure in solution. The former spectrum for each compound showed a 1:1:1:2:2:2 intensity pattern (with one coincidence for **9b**) and with a rather deshielded[12] resonance for B(3) (δ 21.3 (**9a**), 27.3 (**9b**)) that remains a singlet upon retention of proton coupling. Surprisingly, the $^{31}P\{^1H\}$ NMR spectrum showed only a single broad resonance (δ 43.6 (**9a**), 40.8 (**9b**)) for all three PPh_3 ligands, with this showing some possible quartet structure due to unresolved ^2J(BP) coupling to B(3). It may be envisioned that the $\{Au_3(PPh_3)_3\}$ moiety can undergo a "propeller" type of rotation with respect to the metallacarborane surface, which renders the three phosphines equivalent on the NMR time scale, or there may be other, more elaborate fluxional processes taking place. Notably, the related trigold complex [10-*exo*-$\{Au_2(PPh_3)_2\}$-10-*endo*-$\{Au(PPh_3)\}$-7,8-Me_2-*nido*-7,8-$C_2B_9H_8$], which contains a similar $\{Au_3(PPh_3)_3\}$ triangle, also demonstrates fluxional behavior that makes all three PPh_3 groups equivalent and the overall structure symmetric.[31]

As is indicated in Scheme 1, it is thought that initial reaction of compound **2a** or **2b** with $\{Au(PPh_3)\}^+$ results in either (i) addition of the gold fragment, giving compounds of type **6**, or (ii) displacement of the $\{Re(CO)_3\}^+$ moiety and then coordination of two gold units, giving compounds **7**. These suggestions are supported by IR spectroscopic monitoring of the reaction between **2b** and the gold reagent, which at first shows growth of bands attributable to **6b** and **7b**. Notably, reaction of compound **1b** with the same gold substrate also always yield bis-$\{Au(PPh_3)\}$ species (regardless of reaction stoichiometry);[4] it is, therefore, perhaps not surprising that anionic, monogold species ($\{Au-IrCB_9\}^-$ or $\{Au-RhCB_9\}^-$) that would be formal precursors to compounds **7** are not observed in these systems. As the reaction of **2b** with $\{Au(PPh_3)\}^+$ proceeds, IR spectroscopy indicates a decrease in the quantity of **6b** present and a concomitant increase in that of **8b**. Similarly, compound **7b** also appears to partially convert to **9b**, albeit much more slowly. Moreover, solutions of pure samples of **6b** and **7b** with time show the presence of **8b** and **9b**, respectively, as decomposition products, and, as noted earlier, we have observed experimentally that the former pair can be converted more rapidly to the latter two by addition of further gold reagent. All of these observations are consistent with paths (iii) in Scheme 1, namely, that compounds **8** and **9** are formed from **6** and **7**, respectively, by loss of H^+ and gain of $\{Au(PPh_3)\}^+$. Further support for this is provided by the earlier observation[31] that in a related system the digold−carborane species [9-*exo*-$\{Au(PPh_3)\}$-9-(μ-H)-10-*endo*-$\{Au(PPh_3)\}$-7,8-Me_2-*nido*-7,8-$C_2B_9H_8$] affords the trigold complex [10-*exo*-$\{Au_2(PPh_3)_2\}$-10-*endo*-$\{Au(PPh_3)\}$-7,8-Me_2-*nido*-7,8-$C_2B_9H_8$] upon deprotonation (NaH) and addition of $[AuCl(PPh_3)]$. The alternative possibility, namely, that compounds **7** and **9** are formed from **6** and **8**, respectively, by loss of $\{Re(CO)_3\}^+$ and then coordination of $\{Au(PPh_3)\}^+$ (pathway iv in Scheme 1), cannot entirely be excluded, but we found no

(31) Jeffrey, J. C.; Jelliss, P. A.; Stone, F. G. A. *J. Chem. Soc., Dalton Trans.* **1994**, 25.

Scheme 2. Proposed[10] Mechanism for the *exo* ↔ *endo* Vertex Exchange that Occurs in the Formation of Compounds 2[a]

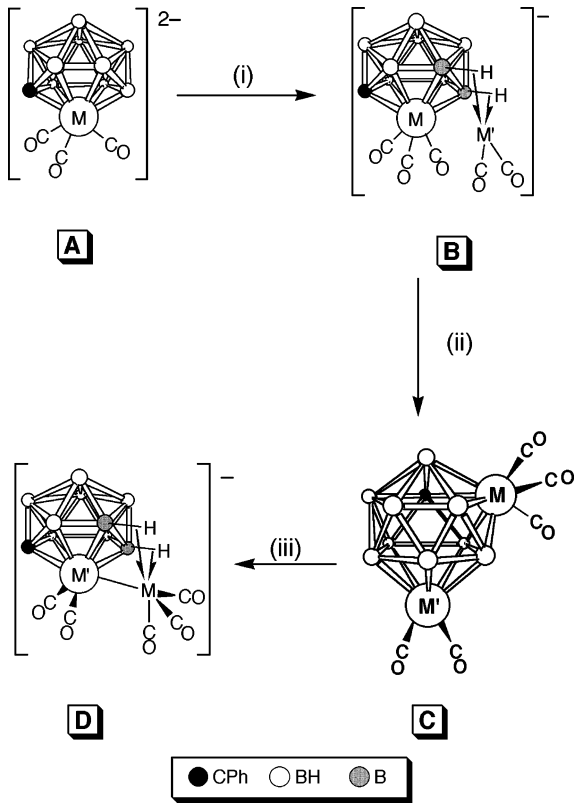

[a] Key: (i) {M′(CO)$_2$} *exo*-coordination; (ii) opening of {MCB$_9$} cluster and then {M′(CO)$_2$} *exo* → *endo* migration; (iii) {M(CO)$_3$} *endo* → *exo* ejection and then {M′CB$_9$} cluster closure.

evidence of this during monitoring of the reactions or by deliberate addition of {Au(PPh$_3$)}$^+$ to the latter pair.

As a final aside, it may be noted that a *closo* ↔ *nido* structural change, similar to that which occurs with compound **6** (i.e., without the expected change in electron count), might also be invoked as part of a possible explanation for the *exo* ↔ *endo* vertex exchange that occurs in the formation of compounds **2** from compounds **1**. This process has been proposed[10] to involve a 12-vertex dimetallacarborane cluster as an intermediate. It is reasonable to assume that the initial step of the latter reaction is simple coordination of the {M′(CO)$_2$}$^+$ fragment to the dianions **A** of compounds **1**, giving the bimetallic MM′ species **B** (see Scheme 2). There is ample precedent for the formation of such structures in other, closely related reactions of compounds **1**.[4,5b] Were the rhena- or manga-carborane cores of **B** to temporarily undergo some kind of *closo* → *nido* cage opening following coordination of the *exo*-polyhedral {M′(CO)$_2$} groups, this could allow the latter to easily migrate from an *exo*- to an *endo*-polyhedral site, giving intermediate **C**. Thereafter, expulsion of the {M(CO)$_3$} vertex and then cage closure would afford the observed products **D**, the anions of compounds **2**, as proposed earlier.[10]

Such a mechanism, of course, is highly speculative and is perhaps also somewhat surprising. Given the known stability of *closo*-12-vertex species with respect to 11-vertex ones,[32] it might not be expected that the transformation **C** → **D** (Scheme 2) would be favorable. However, we have earlier reported that a {PtMnCB$_9$} cluster that is a direct analogue of structure **C** does indeed expel a manganese fragment.[5b] Moreover, it is increasingly being suggested that established cluster stability patterns may not always strictly apply, especially when multiple metal vertexes are present. It should be remembered also that species such as that in structure **C** are one bonding electron pair short of the conventional *closo* electron count,[18−20] and this will certainly have an effect on their relative stabilities. Our efforts continue in trying to understand the processes involved in these and related reactions.

(32) Schleyer, P. v. R.; Najafian, K.; Mebel, A. M. *Inorg. Chem.* **1998**, *37*, 6765.

Conclusion

The surprising formation of compounds **2** from their precursors **1**, via *exo* ↔ *endo* exchange of {metal−ligand} vertexes, was described in the accompanying paper[10] and is itself a remarkable and highly significant observation in metallacarborane chemistry. However, those reactions notwithstanding, arguably the most important aspect of the behavior of compounds **2** is their reactions with copper− and gold−phosphine cations reported herein, with several of the resulting products revealing structures without close precedent in either metallacarborane or metal cluster chemistry. Moreover, we have demonstrated the utility of monocarborane ligands to function as scaffolds for the stepwise addition of different metal centers, leading to a variety of heteropolymetallic products that culminate in the "butterfly" species **8**. There may also be other, as yet undetected, products or intermediates present in all of these reactions: their isolation and identification may help to shed light upon the processes taking place. Clearly much work remains to be done in order to fully understand the formation of compounds **2** from compounds **1** and the subsequent synthesis of the heteropolymetallic species reported herein. There is also much further scope within this area, exploiting other combinations of {metal−ligand} fragments and by employing the many other new monocarboranes that have recently become available.[3]

Experimental Section

General Considerations. All reactions were performed under an atmosphere of dry, oxygen-free dinitrogen using standard Schlenk-line techniques. Solvents were stored over and freshly distilled from appropriate drying agents prior to use. Petroleum ether here refers to that fraction of boiling point 40−60 °C. Chromatography columns (typically ca. 15 cm in length and ca. 2 cm in diameter) were packed with silica gel (Acros, 60−200 mesh). Filtrations through Celite typically employed a plug ca. 5 cm in depth. Preparative thin-layer chromatography (TLC) was performed on 20 × 20 cm glass plates (Uniplates with tapered thickness silica gel GF$_{254}$, Analtech). Elemental analyses were performed by Atlantic Microlab, Inc., Norcross, GA, on crystalline or microcrystalline samples that had been dried overnight in vacuo. On occasion residual solvent remained after drying, its presence and approximate proportion confirmed by integrated ^{1}H NMR spectroscopy, and this was factored into the calculated microanalysis data. NMR spectra were recorded at the following frequencies (MHz): ^{1}H, 360.1; ^{13}C, 90.6; ^{11}B, 115.5; ^{31}P, 145.8. Complexes **2a**,[10] **2b**,[10] [CuCl(PPh$_3$)]$_4$,[33] and [AuCl(PPh$_3$)][34] were prepared by literature methods. All other materials were used as received. For purposes of comparison, product yields are quoted on the basis of the starting compound **2a** or **2b**: in all reactions, up to 20% or 50% of compound **3a** or **3b**, respectively, is also formed as an unavoidable side-product.

(33) Jardine, F. H.; Rule, J.; Vohra, G. A. *J. Chem. Soc. A* **1970**, 238.
(34) Bruce, M. I.; Nicholson, B. K.; Bin Shawkataly, O. *Inorg. Synth.* **1989**, *26*, 325.

Table 4. Crystallographic Data for 5a, 6b, 7b, 8b, and 9b

	5a·$(CH_3)_2CO$	**6b**·$0.5CH_2Cl_2$	**7b**·$0.5CH_2Cl_2$	**8b**·C_5H_{12}	**9b**
formula	$C_{48}H_{50}B_9Cu_2IrO_3P_2$	$C_{30.5}H_{30}AuB_9ClO_5PReRh$	$C_{45.5}H_{45}Au_2B_9ClO_2P_2Rh$	$C_{53}H_{55}Au_2B_9O_5P_2ReRh$	$C_{63}H_{58}Au_3B_9O_2P_3Rh$
fw	1153.39	1126.33	1315.34	1614.24	1731.10
space group	$P2_1/c$	$P\bar{1}$	$P2_1/n$	$P2_1/n$	$P2_1/c$
a, Å	16.9819(15)	10.9430(12)	13.2293(7)	18.6109(15)	18.7506(15)
b, Å	14.8312(13)	13.5989(14)	18.9707(10)	17.0445(15)	12.7722(15)
c, Å	19.6220(15)	14.2374(18)	19.1492(11)	19.674(2)	25.442(2)
α, deg	90	106.139(6)	90	90	90
β, deg	91.699(5)	109.551(6)	100.396(2)	115.685(3)	94.055(4)
γ, deg	90	103.083(6)	90	90	90
V, Å^3	4939.9(7)	1794.5(4)	4727.0(4)	5624.1(9)	6077.8(10)
Z	4	2	4	4	4
ρ_{calcd}, g cm^{-3}	1.551	2.084	1.848	1.906	1.892
μ(Mo Kα), mm^{-1}	3.645	8.054	6.699	7.736	7.608
no. of rflns measd	132 852	23 821	38 586	65 525	40 134
no. of indep rflns	18 945	7159	10 730	15 647	12 169
R_{int}	0.0383	0.0633	0.0950	0.1164	0.1013
wR_2, R_1[a] (all data)	0.0627, 0.0400	0.0938, 0.0596	0.1184, 0.1224	0.0942, 0.1279	0.0838, 0.1069
wR_2, R_1 (obsd[b] data)	0.0580, 0.0264	0.0842, 0.0392	0.1022, 0.0618	0.0776, 0.0510	0.0698, 0.0522

[a] $wR_2 = [\sum\{w(F_o^2 - F_c^2)^2\}/\sum w(F_o^2)^2]^{1/2}$; $R_1 = \sum||F_o| - |F_c||/\sum|F_o|$. [b] $F_o > 4\sigma(F_o)$.

Reaction of 2a or 2b with {Cu(PPh$_3$)}$^+$. (i) To compound **2a** (0.100 g, 0.08 mmol), $[CuCl(PPh_3)]_4$ (0.029 g, 0.02 mmol), and $Tl[PF_6]$ (0.028 g, 0.08 mmol) was added CH_2Cl_2 (20 mL) and the resultant mixture stirred overnight. The mixture was filtered (Celite), and the filtrate was evaporated in vacuo. Column chromatography, eluting first with CH_2Cl_2−petroleum ether (1:1), removed a pale yellow band from which was obtained [1,4,7-{Cu(PPh$_3$)}-1,5,6-{Re(CO)$_3$}-4,5,6,7-(μ-H)$_4$-1,1-(CO)$_2$-2-Ph-*closo*-1,2-IrCB$_9$H$_5$] (**4a**; 0.010 g) as pale yellow microcrystals after removal of solvent in vacuo. Further elution with CH_2Cl_2−petroleum ether (2:1) gave a yellow band, which afforded [1,3,6-{Cu$_2$(PPh$_3$)$_2$}-3,6-(μ-H)$_2$-1,1-(CO)$_2$-2-Ph-*closo*-1,2-IrCB$_9$H$_7$] (**5a**; 0.036 g) as a yellow, microcrystalline solid after evaporation in vacuo.

(ii) Compound **2b** (0.200 g, 0.17 mmol) and $[CuCl(PPh_3)]_4$ (0.063 g, 0.04 mmol) were dissolved in CH_2Cl_2 (20 mL), and finely ground $Tl[PF_6]$ (0.062 g, 0.18 mmol) was added. The mixture was stirred vigorously for 1 h and then evaporated in vacuo. The dark orange residue was extracted with CH_2Cl_2−petroleum ether (1:1, 5 mL), and the extract filtered (Celite) and applied to a chromatography column. Elution with CH_2Cl_2−petroleum ether (3:2) afforded a golden yellow band that gave, after removal of solvent in vacuo, crude [1,3,6-{Cu$_2$(PPh$_3$)$_2$}-3,6-(μ-H)$_2$-1,1-(CO)$_2$-2-Ph-*closo*-1,2-RhCB$_9$H$_7$] (**5b**). This was purified by further column chromatography, eluting with the same solvent mixture, to give **5b** (0.038 g) as a yellow microcrystalline solid.

Reaction of 2a or 2b with {Au(PPh$_3$)}$^+$. (i) To compound **2a** (0.100 g, 0.08 mmol), [AuCl(PPh$_3$)] (0.040 g, 0.08 mmol), and $Tl[PF_6]$ (0.030 g, 0.08 mmol) was added CH_2Cl_2 (20 mL) and the mixture stirred overnight. The mixture was filtered (Celite) and solvent removed from the filtrate by evaporation in vacuo. The residue was subjected to column chromatography, eluting first with CH_2Cl_2−petroleum ether (1:1), to give an orange band that was collected and evaporated in vacuo to furnish [1,3,6-{Au$_2$(PPh$_3$)$_2$-Re(CO)$_3$}-6-(μ-H)-1,1-(CO)$_2$-2-Ph-*closo*-1,2-IrCB$_9$H$_7$] (**8a**; 0.021 g) as orange microcrystals. Thereafter, elution with CH_2Cl_2−petroleum ether (2:1) gave a yellow fraction from which was likewise obtained [1,6-{Au$_2$(PPh$_3$)$_2$}-6-(μ-H)-1,1-(CO)$_2$-2-Ph-*closo*-1,2-IrCB$_9$H$_8$] (**7a**; 0.042 g) as a yellow, microcrystalline solid.

(ii) A similar reaction, employing **2a** (0.100 g, 0.08 mmol), [AuCl(PPh$_3$)] (0.080 g, 0.16 mmol), and $Tl[PF_6]$ (0.060 g, 0.17 mmol), upon column chromatographic workup gave **8a** (0.013 g; 10%) and then a yellow fraction containing a mixture of **7a** and [1,3-{Au$_3$(PPh$_3$)$_3$}-1,1-(CO)$_2$-2-Ph-*closo*-1,2-IrCB$_9$H$_8$] (**9a**). The latter mixture was collected, evaporated, and then applied to preparative TLC plates. Elution with CH_2Cl_2−petroleum ether (1:1) afforded two bright yellow bands that yielded **7a** (R_f = 0.75; 0.011 g; 10%) and **9a** (R_f = 0.35; 0.019 g; 13%), both as microcrystalline yellow solids.

(iii) Compound **2b** (0.200 g, 0.17 mmol) and [AuCl(PPh$_3$)] (0.085 g, 0.17 mmol) were dissolved in CH_2Cl_2 (20 mL), and finely ground $Tl[PF_6]$ (0.062 g, 0.18 mmol) was added. The mixture was stirred vigorously for 1 h and then evaporated in vacuo. The dark orange residue was extracted with CH_2Cl_2−petroleum ether (1:1, 5 mL), and the extract filtered (Celite) and applied to a chromatography column. Elution first with CH_2Cl_2−petroleum ether (4:7) afforded a golden yellow-orange band, which was collected and evaporated in vacuo to afford orange microcrystals of [8,9,10-*endo*-{Au(PPh$_3$)}-3,4,8-*exo*-{Re(CO)$_3$}-3,4-(μ-H)$_2$-8,8-(CO)$_2$-7-Ph-*nido*-8,7-RhCB$_9$H$_7$] (**6b**; 0.017 g). Further elution, using CH_2Cl_2−petroleum ether (2:3), gave a red band that yielded, after removal of solvent in vacuo, crimson microcrystals of [1,3,6-{Au$_2$(PPh$_3$)$_2$Re(CO)$_3$}-6-(μ-H)-1,1-(CO)$_2$-2-Ph-*closo*-1,2-RhCB$_9$H$_7$] (**8b**; 0.018 g). Finally, elution with CH_2Cl_2−petroleum ether (1:1) gave a yellow fraction, which was collected and evaporated in vacuo to give [1,6-{Au$_2$(PPh$_3$)$_2$}-6-(μ-H)-1,1-(CO)$_2$-2-Ph-*closo*-1,2-RhCB$_9$H$_8$] (**7b**; 0.012 g) as a yellow, microcrystalline solid.

(iv) Similarly, compound **2b** (0.100 g, 0.09 mmol), [AuCl(PPh$_3$)] (0.085 g, 0.17 mmol), and $Tl[PF_6]$ (0.060 g, 0.17 mmol) were stirred (16 h) in CH_2Cl_2 (20 mL). Evaporation of the reaction mixture and then column chromatography, eluting with CH_2Cl_2−petroleum ether (1:1), afforded only a single, broad yellow band, which was collected and evaporated to dryness. The residue was purified by preparative TLC, eluting with the same solvent mixture, to give two yellow bands, which were collected and evaporated in vacuo to give **7b** (R_f = 0.70; 0.008 g; 7%) and [1,3-{Au$_3$(PPh$_3$)$_3$}-1,1-(CO)$_2$-2-Ph-*closo*-1,2-RhCB$_9$H$_8$] (**9b**; R_f = 0.35; 0.007 g; 5%), both as golden yellow microcrystalline solids.

X-ray Crystallographic Structure Determinations. Experimental data for the structural studies discussed in the text are presented in Table 4. Data for compounds **4a** and **9a**, and a revised structure of **8a**,[11] are available as Supporting Information only. X-ray intensity data were collected at 110(2) K on a Bruker-Nonius X8 APEX CCD area-detector diffractometer using Mo Kα X-radiation. Several sets of narrow data "frames" were collected at different values of θ, for various initial values of ϕ and ω, using 0.5° increments of ϕ or ω. The data frames were integrated using SAINT;[35] the substantial redundancy in data allowed an empirical absorption correction (SADABS)[35] to be applied, based on multiple measurements of equivalent reflections.

(35) *APEX 2*, version 1.0; Bruker AXS: Madison, WI, 2003−2004.

All structures were solved using conventional direct methods[35,36] and refined by full-matrix least-squares on all F^2 data using SHELXTL version 6.12,[36] with anisotropic thermal parameters assigned to all non-H atoms. The locations of the cage-carbon atoms were verified by examination of the appropriate internuclear distances and the magnitudes of their isotropic thermal displacement parameters. Cluster BH hydrogens for compounds **5a**, **6b**, and **8b** were largely allowed positional refinement, and all other H atoms were set riding in calculated positions, except for a few B−H units that had to be restrained to sensible distances (1.12(5) Å; DFIX card in SHELXL[36]). All hydrogens had fixed isotropic thermal parameters defined as $U_{iso}(H) = 1.2U_{iso}(parent)$, or $U_{iso}(H) = 1.5U_{iso}(parent)$ for methyl groups.

The asymmetric fraction of crystals of **5a** contained one molecule of acetone as solvate, and molecules of **8b** cocrystallized with one molecule of *n*-pentane as solvate, both of these solvates being in general space. Crystals of **6b** contained one-half molecule of CH_2Cl_2 solvate located at an inversion center. All of these solvates were treated straightforwardly as above. The crystals of **7b** also contained one-half molecule of CH_2Cl_2 located at an inversion center, but in this case the crystallographically independent chlorine atom was disordered over two positions. The latter was refined in separate parts with refining complementary occupancies that converge at the approximate ratio 69:31. In addition, in **5a** one of the phenyl rings bonded to P(1) was disordered over two sites. These were treated as two separate parts with refining complementary occupancies, in the approximate ratio 61:39 at convergence.

(36) *SHELXTL*, version 6.12; Bruker AXS: Madison, WI, 2001.

Acknowledgment. We thank the Robert A. Welch Foundation for support (Grant AA-0006) and Dr. Jason A. Kautz for early crystallographic studies in this area. The Bruker-Nonius X8 APEX diffractometer was purchased with funds received from the National Science Foundation Major Instrumentation Program (Grant CHE-0321214).

Supporting Information Available: Full details of the crystal structure analyses (including data for compounds **4a**, **8a**, and **9a**) in CIF format. This material is available free of charge via the Internet at http://pubs.acs.org.

OM060418R